Available online at www.sciencedirect.com

ScienceDirect

IFAC Papers Online CONFERENCE PAPER ARCHIVE

IFAC PapersOnLine 51-29 (2018) 305–310

Path Planning for Marine Vehicles using Bézier Curves

Vahid Hassani [*,**,1] **Simen V. Lande** [*]

[*] *Centre for autonomous marine operations and systems (AMOS) and Dept. of Marine Technology, Norwegian Univ. of Science and Technology, Trondheim, Norway.*

[**] *SINTEF Ocean, formerly Known as Norwegian Marine Technology Research Institute (MARINTEK), Trondheim, Norway.*

Abstract: Over the past few years maritime sector has witnessed an increasing interest in use of autonomous ships and in particular Autonomous Surface Vehicles (ASV) in complex applications with high associated risks. There is an uprising interest in the development of advanced path planning algorithms for marine vehicles in congested waterways. Availability of an efficient path planning technique that considers the dynamic capabilities of the vehicle is of paramount importance in the implementation of these algorithms. This article reports an early work which aims to contribute to the development of a new generation of path planning that incorporates in its formulation the dynamics of the vehicles and extra data made available by on board sensors about obstacles and other vehicles in vicinity. To this end, Bézier Curves are exploited as the basis for generating a rich set of paths. Then, differential flatness property of the vehicle is used to assign a cost function to each path that reflects the dynamic capabilities of the vehicle on that path. The efficacy of the proposed algorithm is shown by help of numerical simulations.

Keywords: Bézier curve, path planning, differential flatness

1. INTRODUCTION

One of the earliest path planning algorithms goes back to the early 1950s, where Claude Shannon and his wife, Betty Shannon, built a three wheel magnetic mouse that could find its path through an electro-mechanical maze (MIT Museum, 1952). Theseus maze was a visual display of path planing in dial telephone systems. It showed how information would travel to find the right target telephone to ring when a phone call is made. The problem of connecting two points on the map in presence of obstacles and forbidden zones found many industrial applications. Different techniques were developed to address the path planning problem. The literature on path planning is vast and interested reader is referred to (Laumond, 1998; McLain and Beard, 2000; LaValle, 2006; Kaminer et al., 2006; Dadkhah and Mettler, 2012; Bhushan Mahajan, 2013; Lekkas, 2014) and references therein. Furthermore, assessing the efficacy of path planning algorithms for different applications is a challenging task and out of the scope of this article; see (Dadkhah and Mettler, 2012; Lekkas, 2014) for some guideline on evaluating different path planning algorithms.

(Hausler et al., 2009) gives an introductory application example where a group of autonomous marine vehicles, spread at arbitrary positions and headings, are to perform a cooperative mission at sea that requires adopting a predefined geometrical formation pattern. The vehicles should sail from their initial position and arrive at the final formation pattern at the same time. They call this as "Go-To-Formation" maneuver which, due to existence of obstacles, restricted areas, and required safety distance from other vehicles, needs an advanced path planning algorithm. The different challenges that should be addresses in course of solving Go-To-Formation problem are listed in (Hausler et al., 2009) and later in (Häusler et al., 2010).

Path planing for marine vehicles inherits an increasingly complexity and challenging requirements. Development of autonomous ships and increasing applications for multiple vehicle coordination have created a widespread interest in the development of advanced path planning algorithms for marine vehicles in congested waterways (LaValle, 2006; Hausler et al., 2009; Häusler et al., 2009, 2010).

(Hausler et al., 2009; Ghabcheloo et al., 2009), borrowing the tools introduced by (Yakimenko, 2000; Kaminer et al., 2006), used a group of 5th order polynomial paths as basis for their path generation algorithm. The coefficient of the polynomials were computed such that the boundary conditions such as initial and final position and heading were met. Their methodology generates paths that completely govern spatial profile of the vehicles. A second temporal problem is solved to address the de-confliction in time to reduce the risk of collision between vehicles and speed assignment for simultaneous arrival of all the vehicles to their final formation pattern.

⋆ This work was supported by Centre for autonomous marine operations and systems (AMOS); the Norwegian Research Council is acknowledged as the main sponsor of AMOS.

[1] Corresponding author, (e-mail: Vahid.Hassani@ntnu.no).

10.1016/j.ifacol.2018.09.520

Motivated by the above considerations, this article reports results of an early work which aims to contribute to the development of a new generation of path planning that incorporates in its formulation the dynamics of the vehicles and extra data made available by on board sensors about obstacles and other vehicles in vicinity. In this paper, Bézier Curves are used as the basis for generating a rich set of paths that determines spatial and temporal profile of the vehicles. Using differential flatness property of the vehicle, we are able to reconstruct all the states of the vehicles during the maneuver. The calculated states are then used to assign a cost function to each path that reflects the dynamic capabilities of the vehicle on that path.

The rest of the article is organized as follows. Section 2 presents a brief introduction to Bézier curves. Section 3 describes the key idea behind the proposed path generation technique. It also provides a summary of differential flatness theory and studies how one can assign a cost to each path such that it reflects the dynamic behaviour of the vehicle. In section 4, a short description of the optimization algorithm is presented. Numerical simulation results of the proposed technique are presented in Section 5. Conclusions and suggestions for future research are summarized in Section 6.

2. BÉZIER CURVE

The mathematical basis for the Bézier curve are the Bernstein polynomials, named after the Russian mathematician Sergei Natanovich Bernstein (Farin, 2014). In 1912 the Bernstein polynomials were first introduced and published as a means to constructively prove the Weierstrass theorem. In other words, as the ability of polynomials to approximate any continuous function, to any desired accuracy over a given interval. The slow convergence rate and the technological challenges in the construction of the polynomials at the time of publication, led to the Bernstein polynomial basis being seldom used for several decades to come. Around the 1960s, independently, two French automobile engineers of different companies, started searching for ways of representing complex shapes, such as automobile bodies using digital computers. The motivation for finding a new way to represent free-form shapes at the time, was due to the expensive process of sculpting such shapes, which was done using clay. The first engineer concerned with this matter was Paul de Faget de Casteljau working for Citroën, who did his research in 1959. His findings lead to what is known as de Casteljau's algorithm, a numerically stable method to evaluate Bézier curves. De Casteljau's work were only recorded in Citroën's internal documents, and remained unknown to the rest of the world for a long time. His findings are however today, a great tool for handling Bézier curves (Farin, 2014). The person who lends his name to the Bézier curves, and is principally responsible for making the curves so well known, is the engineer Pierre Ètienne Bézier. Bézier worked at Renault, and published his ideas extensively during the 1960s and 1970s. Both Bézier's and de Casteljau's original formulations did not explicitly invoke the Bernstein basis, however the key features are unmistakably linked to it and today the Bernstein basis is a key part in the formulation (Farouki, 2012).

A Bézier curve is defined by a set of control points $\boldsymbol{P}_i$ $(i = 0 \dots n)$ for which n denotes the degree of the curve. The number of control points for a curve of degree n is $n+1$, and the first and last control points will always be the end points of the curve. The intermediate points does not necessarily lay on the curve itself. The Bézier curve can be express on a general form as

$$\boldsymbol{P}(t) = \sum_{i=0}^{n} B_i^n(t)\boldsymbol{P}_i \quad t \in [0,1] \tag{1}$$

here t defines a normalized time variable and $B_i^n(t)$ denotes the blending functions of the Bézier curve, which are Bernstein polynomials defined as

$$B_i^n = \binom{n}{i}(1-t)^{n-i}t^i, \quad i = 0, 1, 2..., n \tag{2}$$

2.1 Derivatives

The derivative of any Bézier curve of degree n is a Bézier curve of degree $n-1$. As the control points are constant and independent of the curve parameter t, the derivative is found by computing the derivative of the Bernstein polynomials. The first derivative for the Bernstein polynomials given by Eq.(2) are

$$\dot{B}_i^n(t) = n(B_{i-1}^{n-1}(t) - B_i^{n-1}(t)). \tag{3}$$

The derivative of the Bézier curve then takes the following form

$$\dot{\boldsymbol{P}}(t) = n\sum_{i=0}^{n-1} B_i^{n-1}(t)(\boldsymbol{P}_{i+1} - \boldsymbol{P}_i) \quad t \in [0,1]. \tag{4}$$

To further simplify this expression we can define the control points of the first derivative as $\boldsymbol{Q}_i = \boldsymbol{P}_{i+1} - \boldsymbol{P}_i$, the expression then takes the following form

$$\dot{\boldsymbol{P}}(t) = n\sum_{i=0}^{n-1} B_i^{n-1}(t)\boldsymbol{Q}_i \quad t \in [0,1]. \tag{5}$$

Higher order derivatives can be found by repeated use of the relation described in Eq.(3) and Eq.(5).

2.2 Curvature

The curvature of a Bézier curve, given by $\boldsymbol{P}(t) = (x(t), y(t))$, can be expressed in the following form

$$\kappa(t) = \frac{\dot{x}(t)\ddot{y}(t) - \ddot{x}(t)\dot{y}(t)}{(\dot{x}(t)^2 + \dot{y}(t)^2)^{\frac{3}{2}}}. \tag{6}$$

This expression is known as the signed curvature as it takes both positive and negative values. The sign of the curvature will indicate the direction in which the unit tangent vector rotates, as a function of the parameter t along the curve.

3. DIFFERENTIAL FLATNESS

In this section, using the description of differential flatness presented in (Van Nieuwstadt and Murray, 1998), an informal definition of differential flatness will be presented. A system is said to be differentially flat if one can find a set of outputs, equal in number to the number of inputs, such that one can express all states and inputs as functions of these outputs and their derivatives. This can be formulated mathematically for a nonlinear system, as follows. Consider a nonlinear system

$$\dot{x} = f(x,u) \quad x \in \mathbb{R}^n,\ u \in \mathbb{R}^m \tag{7}$$
$$y = h(x) \qquad y \in \mathbb{R}^m, \tag{8}$$

where x denotes the state vector, u denotes the control input vector and y denotes the tracking output vector.

Such a system is said to be differentially flat if there exist a vector $z \in \mathbb{R}^m$, known as the flat output, of the form

$$z = \zeta(x, u, \dot{u}, ..., u^{(r)}), \tag{9}$$

such that

$$x = \phi(y, \dot{y}, ..., y^{(q)}) \tag{10}$$
$$u = \alpha(y, \dot{y}, ..., y^{(q)}), \tag{11}$$

where ζ, ϕ and α are smooth functions.

3.1 Model of Surface Vessel

The mathematical model of the surface vessel motion is described by the kinematics and the dynamics as (Fossen, 2011)

$$\begin{aligned} \dot{\boldsymbol{\eta}} &= \boldsymbol{R}(\psi)\boldsymbol{\nu} \\ \boldsymbol{M}\dot{\boldsymbol{\nu}} + \boldsymbol{C}(\boldsymbol{\nu})\boldsymbol{\nu} + \boldsymbol{D}\boldsymbol{\nu} &= \boldsymbol{\tau}, \end{aligned} \tag{12}$$

where $\boldsymbol{\eta} = [x, y, \psi]^T$ denotes the position and orientation in the earth fixed coordinates, $\boldsymbol{\nu} = [u, v, r]^T$ denotes the generalized velocity given in the body-fixed frame and $\boldsymbol{\tau} = [\tau_1, 0, \tau_3]$ represents the control forces. Further, $\boldsymbol{R}(\psi)$ is the rotation matrix, $\boldsymbol{M}$ is constant positive-definite matrix representing the inertia of the vessel, and $\boldsymbol{C}(\boldsymbol{\nu})$ is the Coriolis and centripetal matrix. The term $\boldsymbol{D}$ represents the linear damping matrix. Specifically, these matrices are given as

$$\boldsymbol{R}(\psi) = \begin{bmatrix} \cos(\psi) & -\sin(\psi) & 0 \\ \sin(\psi) & \cos(\psi) & 0 \\ 0 & 0 & 1 \end{bmatrix}, \tag{13}$$

$$\boldsymbol{C}(\boldsymbol{\nu}) = \begin{bmatrix} 0 & 0 & -m_{22}v \\ 0 & 0 & m_{11}u \\ m_{22}v & -m_{11}u & 0 \end{bmatrix}, \tag{14}$$

$$\boldsymbol{M} = \mathrm{diag}\{m_{11}, m_{22}, m_{33}\}, \tag{15}$$
$$\boldsymbol{D} = \mathrm{diag}\{d_{11}, d_{22}, d_{33}\}. \tag{16}$$

This paper will consider a simplified version of the underactuated ship model, by enforcing the following simplifications

$$m_{11} = m_{22}, \quad \beta_1 = \frac{d_{11}}{m_{11}}, \quad \beta_2 = \frac{d_{22}}{m_{22}},$$
$$\beta_3 = \frac{d_{33}}{m_{33}}, \quad \tau_u = \frac{\tau_1}{m_{11}}, \quad \tau_r = \frac{\tau_3}{m_{33}}.$$

Rearranging the vehicle dynamics in (12), the state space representation of the underactuated surface vessel follows the following form

$$\dot{x} = u\cos(\psi) - v\sin(\psi) \tag{17}$$
$$\dot{y} = u\sin(\psi) + v\cos(\psi) \tag{18}$$
$$\dot{\psi} = r \tag{19}$$
$$\dot{u} = vr - \beta_1 u + \tau_u \tag{20}$$
$$\dot{v} = -ur - \beta_2 v \tag{21}$$
$$\dot{r} = -\beta_3 r + \tau_r. \tag{22}$$

In what follows, we show that the model described above is differentially flat. we furthermore, calculate the flat outputs of the system.

Choosing the flat outputs for the system model as the coordinates of the vessel in the North-East plane, we show that all the states can be found using the selected flat outputs.

$$\boldsymbol{z} = [z_1,\ z_2] = [x,\ y]. \tag{23}$$

In order to prove flatness for the system, we will first express the derivatives of Eq. (17) and Eq. (18) as

$$\ddot{x} = (\dot{u} - v\dot{\psi})\cos(\psi) - (\dot{v} + u\dot{\psi})\sin(\psi) \tag{24}$$
$$\ddot{y} = (\dot{v} + u\dot{\psi})\cos(\psi) + (\dot{u} - v\dot{\psi})\sin(\psi). \tag{25}$$

Furthermore, by the use of Eq. (20) and Eq. (21), we can prove that the following holds

$$\ddot{x} + \beta_2\dot{x} = (\beta_u u + \tau_u)\cos(\psi) \tag{26}$$
$$\ddot{y} + \beta_2\dot{y} = (\beta_u u + \tau_u)\sin(\psi), \tag{27}$$

where $\beta_u := \beta_2 - \beta_1$. By using these two expressions, we obtain the following relation

$$\psi = \tan^{-1}\left(\frac{\ddot{y} + \beta_2\dot{y}}{\ddot{x} + \beta_2\dot{x}}\right). \tag{28}$$

Thus, Eq. (28) proves that ψ can be written as a function of the flat output and its derivatives.

From Eq. (17) and Eq. (18), we obtain

$$u = \dot{x}\cos(\psi) + \dot{y}\sin(\psi) \tag{29}$$
$$v = \dot{y}\cos(\psi) - \dot{x}\sin(\psi). \tag{30}$$

Using the above equations, and Eq. (28) we obtain

$$u = \frac{\dot{x}(\ddot{x} + \beta_2\dot{x}) + \dot{y}(\ddot{y} + \beta_2\dot{y})}{\sqrt{(\ddot{x} + \beta_2\dot{x})^2 + (\ddot{y} + \beta_2\dot{y})^2}} \tag{31}$$

and

$$v = \frac{\dot{y}\ddot{x} - \dot{x}\ddot{y}}{\sqrt{(\ddot{x} + \beta_2\dot{x})^2 + (\ddot{y} + \beta_2\dot{y})^2}}. \quad (32)$$

Using Eq. (22) and Eq. (28) it can be shown that the following holds

$$r = \frac{(y^{(3)} + \beta_2\ddot{y})(\ddot{x} + \beta_2\dot{x}) - (x^{(3)} + \beta_2\ddot{x})(\ddot{y} + \beta_2\dot{y})}{(\ddot{x} + \beta_2\dot{x})^2 + (\ddot{y} + \beta_2\dot{y})^2}. \quad (33)$$

Thus proving that all the states can be written as functions of the flat output. The task of proving that the control inputs can be written as functions of the flat output becomes trivial, as they can be expressed as functions of the states and the derivatives of the states. Through the use of Eq. (20) and Eq. (22), and the expressions for the states we obtain

$$\tau_u = \frac{(\ddot{x} + \beta_1\dot{x})(\ddot{x} + \beta_2\dot{x}) + (\ddot{y} + \beta_1\dot{y})(\ddot{y} + \beta_2\dot{y})}{\sqrt{(\ddot{x} + \beta_2\dot{x})^2 + (\ddot{y} + \beta_2\dot{y})^2}} \quad (34)$$

and

$$\tau_r = \dot{r} + \beta_3 r \quad (35)$$

where r is given by Eq.(33) and $\dot{r}$ is given as

$$\dot{r} = \frac{(y^{(4)} + \beta_2 y^{(3)})(\ddot{x} + \beta_2\dot{x}) - (x^{(4)} + \beta_2 x^{(3)})(\ddot{y} + \beta_2\dot{y})}{(\ddot{x} + \beta_2\dot{x})^2 + (\ddot{y} + \beta_2\dot{y})^2} - \frac{2\left((y^{(3)} + \beta_2\ddot{y})(\ddot{x} + \beta_2\dot{x}) - (x^{(3)} + \beta_2\ddot{x})(\ddot{y} + \beta_2\dot{y})\right)}{\left((\ddot{x} + \beta_2\dot{x})^2 + (\ddot{y} + \beta_2\dot{y})^2\right)^2}\Big((\ddot{x} + \beta_2\dot{x})(x^{(3)} + \beta_2\ddot{x}) + (\ddot{y} + \beta_2\dot{y})(y^{(3)} + \beta_2\ddot{y})\Big) \quad (36)$$

Before taking the next step in formulating our path planning algorithm, let us take the discussion stage further. Showing the differentially flatness property of the vehicle, allows us by using any Bézier curve and flatness property of the system, assign a cost function to each path using the calculated states of the system along the path. Our formulation at the current stage assumes that there is no side-slip along the path.

4. OPTIMIZATION

In what follows, we formulate our path planning algorithm in an optimization framework. The proposed path planning technique, utilizes optimization in order to generate a feasible path, that accounts for both physical- and workspace constraints. The workspace constraints refers to obstacle and forbidden zones that ship should not sail through. Furthermore, the ship dynamics are accounted for by the use of differential flatness and assigning a cost function to each path based on the computed states of the system along the path.

The path planning program generates a path between two predetermined waypoints, by stitching a set of Bézier curves together such that the heading and curvature along the path remains continuous. Ultimately, this means that the path that is generated is C^2 continuous. Further, we account for workspace constraints, by including a set of static obstacles in the optimization.

In order to successfully generate a reference path for the vehicle we have used 5th-order Bézier curves. This is due to the fact that lower order curves are not able to offer all the properties that we desire such as C^2 continuity.One should note that increasing the degree of the Bézier curves, could also lead to numerical instability (Skrjanc and Klancar, 2007).

The proposed path planing technique uses the control points of the Bézier curves as design variables, and allows one to specify the number of Bézier curves segments m that is to be stitched together in order to generate the path.

4.1 Optimization Constraints

In what follows we briefly describe the set of constraints that are imposed in the optimization problem.

Continuity constraints: In order to obtain continuity in position, heading and curvature the following constraints will be imposed on the path

$$\boldsymbol{P}_{5,i} = \boldsymbol{P}_{0,i+1}, \qquad i \in [1,\, m-1] \quad (37)$$
$$\boldsymbol{P}_{1,i+1} + \boldsymbol{P}_{4,i} = 2\boldsymbol{P}_{5,i}, \qquad i \in [1,\, m-1] \quad (38)$$
$$\boldsymbol{P}_{2,i+1} - 2\boldsymbol{P}_{1,i+1} += \boldsymbol{P}_{3,i} - 2\boldsymbol{P}_{4,i}, \; i \in [1,\, m-1] \quad (39)$$

where the numerals denote the control points and i denotes the curve segment number.

Initial and final conditions: The initial and final conditions for the position can be formulated as constraints as follows

$$\boldsymbol{P}_{0,1} = WP_0, \quad \boldsymbol{P}_{5,m} = WP_1, \quad (40)$$

where WP_0 and WP_1 denotes the position of the endpoints in the north-east plane. The constraint for the initial and final conditions for the heading in these endpoints can be formulated as follows

$$l_0 \begin{bmatrix} \sin(\psi_0) \\ \cos(\psi_0) \end{bmatrix} = 5(\boldsymbol{P}_{1,1} - \boldsymbol{P}_{0,1}), \quad (41)$$
$$l_1 \begin{bmatrix} \sin(\psi_1) \\ \cos(\psi_1) \end{bmatrix} = 5(\boldsymbol{P}_{5,m} - \boldsymbol{P}_{4,m}), \quad (42)$$

where ψ_0 and ψ_1 denotes the heading angle in the first waypoint and the second waypoint, respectively. Furthermore, $l_0, l_1 \in \mathbb{R}^+$ are some positive constants, determining the length of the vector in the two waypoints, respectively. Note that these equations will only constrain the direction of the heading vector in the endpoints, and not the magnitude of the vector. These constraint requires the introduction of l_0 and l_1 as design variables.

Turning radius: To ensure that the path has no turns smaller than the minimum turning radius of the ship, we will impose a constraint on the curvature along the path. This could be formulated as

$$|\kappa(t)| < \kappa_{max} = \frac{1}{R_{min}}, \tag{43}$$

where $\kappa(t)$ is the curvature of the path, R_{min} is the minimum turning radius and κ_{max} is the corresponding maximum curvature.

Static obstacles: Environmental constraints will be included in the optimization as static obstacles. Each obstacle will be represented by a circle with radius r and center in (x, y) in the North-East plane. These constraints will take on the following form

$$r \leq \sqrt{(x(t) - x)^2 + (y(t) - y)^2}, \tag{44}$$

where $x(t)$ and $y(t)$ denote the coordinates of the path.

4.2 Objective function:

Using the differential flatness property, we will define an objective function that minimizes the energy associated with each of the path segments. This is formulated as

$$J = \sum_{i=1}^{m} \left[\int_0^1 \dot{u}_i(t) dt \right] \tag{45}$$

where i denotes the curve segment number and $\dot{u}$ is found by differentiating Eq.(31). Since we are using the the flatness property of the system, this objective function will include the ship dynamics.

We would like to highlight that in this article the main contribution is formulating the path generation problem in an optimization framework and not solving the problem itself. Throughout this article, the overall optimization problem is solved using a general nonlinear programming solver in MATLAB®.

5. SIMULATION RESULTS

In what follows we present a series of numerical simulation to evaluate the efficacy of the proposed algorithm.

First scenario:
Fig. 1 shows the results of the generated path for the following problem:

Initial condition $(x_0, y_0, \psi_0) = (0, 0, 40)$; Final condition $(x_1, y_1, \psi_1) = (1800, 2600, 15)$; Nr. Obstacles = 65; Minimum Radius= 50 (m) and Maximum Radius 80 (m); Min turning radius= 100 (m); Nr. Bézier curves= 8.

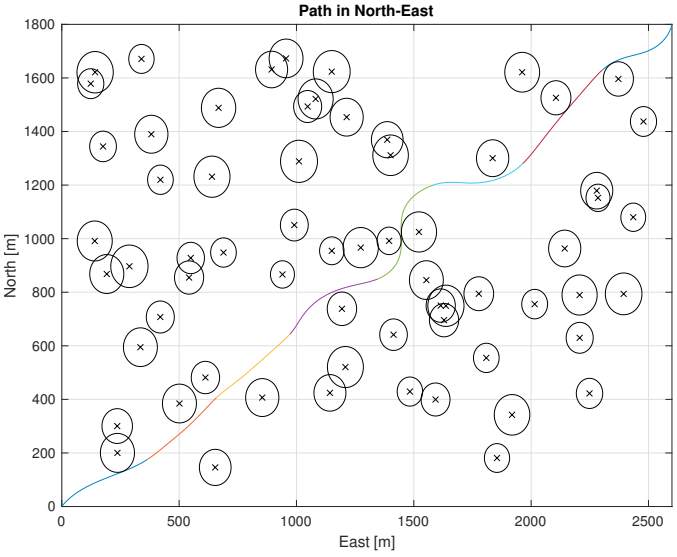

Fig. 1. Graphical representation of the generated path and obstacles in the first scenario

Second scenario:
Fig. 2 shows the results of the generated path for the following problem:

Initial condition $(x_0, y_0, \psi_0) = (0, 0, 35)$; Final condition $(x_1, y_1, \psi_1) = (2000, 2300, 55)$; Nr. Obstacles = 25; Minimum Radius= 70 (m) and Maximum Radius 100 (m); Min turning radius= 100 (m); Nr. Bézier curves= 8.

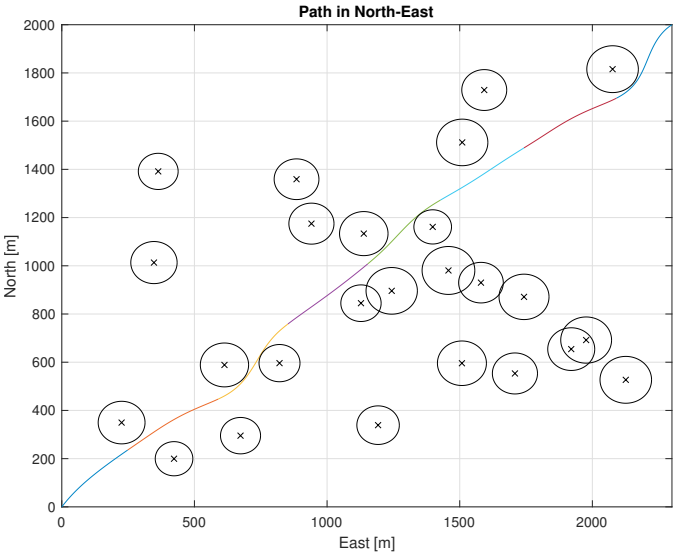

Fig. 2. Graphical representation of the generated path and obstacles in the second scenario

Third scenario:
Fig. 3 shows the results of the generated path for the following problem:

Initial condition $(x_0, y_0, \psi_0) = (0, 0, 90)$; Final condition $(x_1, y_1, \psi_1) = (2000, 2600, 15)$; Nr. Obstacles = 25; Minimum Radius= 70 (m) and Maximum Radius 100 (m); Min turning radius= 100 (m); Nr. Bézier curves= 8.

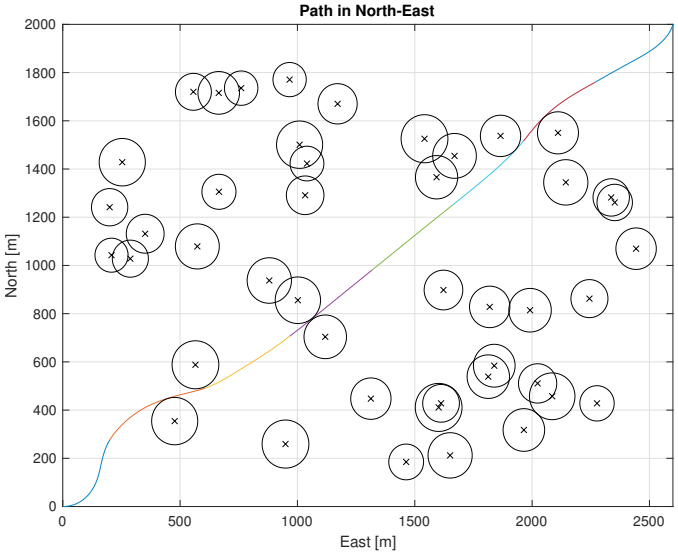

Fig. 3. Graphical representation of the generated path and obstacles in the third scenario

The numerical simulations shows effectiveness of the proposed path planning technique.

6. CONCLUSION

. The problem of path generation for a marine vehicle was addressed in a systematic way. To this end, a class of Bézier curves was used to provide a rich class of potential paths. Using the flatness property of ship, all the states and inputs of the ship along the path was computed from which a cost value was assigned to each candidate path. Finally, an optimization problem was formulated that would give birth to a path that would satisfy all the required properties. The presented work is in its early stage and far from being complete. Future work will include the application of the method developed to multiple vehicles case and development of an efficient optimization technique tailored for the above mentioned problem.

REFERENCES

Bhushan Mahajan, P.M. (2013). Literature review on path planning in dynamic environment. *International Journal of Computer Science and Network*, 2(1).

Dadkhah, N. and Mettler, B. (2012). Survey of motion planning literature in the presence of uncertainty: Considerations for uav guidance. *Journal of Intelligent & Robotic Systems*, 65(1), 233–246. doi:10.1007/s10846-011-9642-9. URL `https://doi.org/10.1007/s10846-011-9642-9`.

Farin, G. (2014). *Curves and surfaces for computer-aided geometric design: a practical guide*. Elsevier.

Farouki, R.T. (2012). The bernstein polynomial basis: A centennial retrospective. *Computer Aided Geometric Design*, 29(6), 379–419.

Fossen, T.I. (2011). Handbook of marine craft hydrodynamics and motion control.

Ghabcheloo, R., Kaminer, I., Aguiar, A.P., and Pascoal, A. (2009). A general framework for multiple vehicle time-coordinated path following control. In *American Control Conference, 2009. ACC'09.*, 3071–3076. IEEE.

Hausler, A.J., Ghabcheloo, R., Kaminer, I., Pascoal, A.M., and Aguiar, A.P. (2009). Path planning for multiple marine vehicles. In *OCEANS 2009-EUROPE*, 1–9. IEEE.

Häusler, A.J., Ghabcheloo, R., Pascoal, A.M., and Aguiar, A.P. (2010). Multiple marine vehicle deconflicted path planning with currents and communication constraints. *IFAC Proceedings Volumes*, 43(16), 491–496.

Häusler, A.J., Ghabcheloo, R., Pascoal, A.M., Aguiar, A.P., Kaminer, I.I., and Dobrokhodov, V.N. (2009). Temporally and spatially deconflicted path planning for multiple autonomous marine vehicles. *IFAC Proceedings Volumes*, 42(18), 376–381.

Kaminer, I., Yakimenko, O., Pascoal, A., and Ghabcheloo, R. (2006). Path generation, path following and coordinated control for timecritical missions of multiple uavs. In *American Control Conference, 2006*, 4906–4913. IEEE.

Laumond, J.P. (ed.) (1998). *Robot motion planning and control*. Springer.

LaValle, S.M. (2006). *Planning algorithms*. Cambridge university press.

Lekkas, A.M. (2014). *Guidance and Path-Planning Systems for Autonomous Vehicles*. Ph.D. thesis, Department of Engineering Cybernetics, Norwegian University of Science and Technology.

McLain, T. and Beard, R. (2000). Trajectory planning for coordinated rendezvous of unmanned air vehicles. In *AIAA Guidance, navigation, and control conference and exhibit*, 4369.

MIT Museum (1952). Theseus Maze. `http://museum.mit.edu/150/20`. Accessed: 2018-03-30.

Skrjanc, I. and Klancar, G. (2007). Cooperative collision avoidance between multiple robots based on bézier curves. In *29th International Conference on Information Technology Interfaces*, 451–456. doi: 10.1109/ITI.2007.4283813.

Van Nieuwstadt, M.J. and Murray, R.M. (1998). Real-time trajectory generation for differentially flat systems. *International Journal of Robust and Nonlinear Control*, 8(11), 995–1020. doi:10.1002/(SICI)1099-1239(199809)8:11¡995::AID-RNC373¿3.0.CO;2-W.

Yakimenko, O.A. (2000). Direct method for rapid prototyping of near-optimal aircraft trajectories. *Journal of Guidance, Control, and Dynamics*, 23(5), 865–875.